




ARTICLE

Prediction of Daily Global Solar Radiation on a Horizontal Plane Using Adaptive Neuro-Fuzzy Inference System (ANFIS)

Hamatti Mohamed¹, Benchrifia Mohammed² , Mohamed Elouardi³ , Mouhsine Hadine³, Mabrouki Jamal^{3*} ,
El-Baz Morad¹, Tadili Rachid⁴

¹ ESMaR, Mohammed V University, Faculty of Sciences, Av. Ibn Battouta, Agdal, Rabat B.P. 1014, Morocco

² Laboratory of Natural Resources and Sustainable Development, Faculty of Sciences, Ibn Tofail University—KENITRA-University Campus, Kenitra 14000, Morocco

³ Laboratory of Spectroscopy, Molecular Modeling, Materials, Nanomaterials, Water and Environment, CERNE2D, Faculty of Science, Mohammed V University in Rabat, Avenue Ibn Battouta, Agdal, Rabat P.O. Box 1014, Morocco

⁴ Laboratory of Solar Energy and Environment, Mohammed V University in Rabat, Faculty

ABSTRACT

In recent years, the world has seen an exponential increase in energy demand, prompting scientists to look for innovative ways to exploit the power sun's power. Solar energy technologies use the sun's energy and light to provide heating, lighting, hot water, electricity and even cooling for homes, businesses, and industries. Therefore, ground-level solar radiation data is important for these applications. Thus, our work aims to use a mathematical modeling tool to predict solar irradiation. For this purpose, we are interested in the application of the Adaptive Neuro Fuzzy Inference System. Through this type of artificial neural system, 10 models were developed, based on meteorological data such as the Day number (N_j), Ambient temperature (T), Relative Humidity (H_r), Wind speed (W_s), Wind direction (W_D), Declination (δ), Irradiation outside the atmosphere (G_{oh}), Maximum temperature (T_{max}), Minimum temperature (T_{min}). These models have been tested by different static indicators to choose the most suitable one for the estimation of the daily global solar radiation. This study led us to choose the M8 model, which takes N_j , T , H_r , δ , W_s , W_d , G_0 , and S_0 as input variables because it

*CORRESPONDING AUTHOR:

Mabrouki Jamal, Laboratory of Spectroscopy, Molecular Modeling, Materials, Nanomaterials, Water and Environment, CERNE2D, Faculty of Science, Mohammed V University in Rabat, Avenue Ibn Battouta, Agdal, Rabat P.O. Box 1014, Morocco; Email: jamalmabrouki@gmail.com

ARTICLE INFO

Received: 18 August 2024 | Revised: 4 September 2024 | Accepted: 29 October 2024 | Published Online: 9 January 2025
DOI: <https://doi.org/10.30564/jees.v7i1.7079>

CITATION

Mohamed, H., Mohammed, B., Elouardi, M., et al., 2025. Prediction of Daily Global Solar Radiation on a Horizontal Plane Using Adaptive Neuro-Fuzzy Inference System (ANFIS). Journal of Environmental & Earth Sciences. 7(1): 527–539. DOI: <https://doi.org/10.30564/jees.v7i1.7079>

COPYRIGHT

Copyright © 2025 by the author(s). Published by Bilingual Publishing Group. This is an open access article under the Creative Commons Attribution-NonCommercial 4.0 International (CC BY-NC 4.0) License (<https://creativecommons.org/licenses/by-nc/4.0/>).

presents the best performance either in the learning phase ($R^2 = 0.981$, $RMSE = 0.107$ kW/m², $MAE = 0.089$ kW/m²) or in the validation phase ($R^2 = 0.979$, $RMSE = 0.117$ kW/m², $MAE = 0.101$ kW/m²).

Keywords: Solar Radiation; Adaptive Neuro-Fuzzy Inference System; Prediction Horizontal Plane; Mathematical Modelling

1. Introduction

The sun produces an enormous amount of energy, which leaves its surface in the form of electromagnetic radiation with a spectrum ranging from 0.2 μm (ultraviolet) to 4 μm (infrared). This energy represents a major source of energy in the future. Despite the considerable distance of the earth from the sun ($150 \cdot 10^6$ km), the earth's surface receives $180 \cdot 10^6$ GW of energy. This makes solar energy a good alternative compared to other energy sources because it represents a considerable potential^[1-4].

The sun derives its energy from the thermonuclear reactions continuously in its core, whose temperature reaches 15 million degrees^[5]. Due to the enormous temperatures and pressures, all matter is in a gaseous or plasma state. The outer layer of the sun, the photosphere, which is visible from the earth, has a considerably lower temperature that decreases towards the outside, to about 5800°K ^[6]. Thermonuclear reactions in the sun's core convert 564 million tonnes of hydrogen into 560 million tonnes of helium every second^[7, 8].

Hydrogen, which accounts for 71% of the mass in the photosphere, is only present at 34% in the central part of the sun, due to this permanent transformation that began 4.5 billion years ago^[9]. The missing 4 million tonnes of mass volatilized and disintegrated in gigantic nuclear explosions. The process involved is well understood since Albert Einstein's famous relation ($E = mc^2$)^[10] which shows that any loss of mass (m) leads to a production of energy equal to the product of this mass and the square of the speed of light. The mass loss of the sun per unit of time is $4.28 \cdot 10^9$ kg/s, and the energy emitted per second by the sun is therefore about $3.85 \cdot 10^{20}$ MW. In terms of energy, a nuclear power plant reactor typically produces 1000 MW. The Sun therefore provides power equivalent to that of 4,1017 nuclear reactors, a truly astronomical figure. However, only a small part of this power is received by the Earth because of the small solid angle at which our planet is seen from the Sun, about two billion times less, which gives a figure that is still quite respectable (about $1.9 \cdot 10^{11}$ MW)^[11-13]. The earth-atmosphere system

reflects about 30% of the intercepted solar energy and absorbs the remaining 70%, which is almost entirely converted into heat. Solar energy is a renewable and inexhaustible energy. This energy can be converted into electrical or thermal energy and can be the solution to the energy challenges of several countries.

Thanks to Morocco's geographical location, the duration of sunshine recorded over the country exceeds 3000 hours annually, and the daily amount of energy received on the ground is about 5 kWh/m², which favors the use of solar energy in different fields such as electricity production by photovoltaic collector^[14-22]. Therefore, knowledge of this radiation is of significant interest in designing and dimensioning solar energy systems. To predict solar energy, we need new techniques like artificial neural networks. In 1948, two American researchers, Mac Culloch and Pitts, gave birth to the first mathematical model of the biological neuron: the formal neuron^[23].

It is clear that Morocco, through its new energy policy, tends to promote the development of renewable energies, particularly solar energy, because of its geographical location, which has one of the highest solar deposits in the world^[24]. However, the exploitation of this solar energy source presents certain technical challenges because of its intermittent and random nature, where its integration into the exploitation networks (electrical or thermal) poses problems for the maintenance of the production-consumption balance. Therefore, efficient use of this solar energy requires reliable forecasting information.

In fact, solar irradiance values are an essential parameter for many applications, such as the dimensioning and performance evaluation of solar thermal and photovoltaic systems. They are also an indispensable element for researchers and engineers in pre-project studies and the development of new systems, as well as in the simulation of new prototypes. However, this data is not always available, especially in isolated locations. Indeed, in such cases, predicting solar irradiance values is the only way to acquire these data. This situation, and also the lack of previous work on solar radiation prediction by ANFIS networks in Morocco, motivated

us to take up the challenge of carrying out the present work.

The current challenge for researchers is to develop predictive models that achieve good performance with a significant reduction in the error rate for different time scales (minute, hourly, daily or monthly). Artificial neural networks have attracted the attention of a large number of researchers in the field of renewable energy, and in particular for the prediction of meteorological data such as solar irradiation^[25–29]. Indeed, many research works have proven the ability of neural networks to predict weather data. They have shown that they are more suitable, and give better results compared to conventional approximation methods proposed by other researchers, for the prediction of solar irradiation. The advantage of the proposed methodology (modeling by artificial neural networks) is that it offers the possibility of implicitly exploiting the information associated with the problem, without having an a priori knowledge of the relationship between the different variables and solar irradiation.

The objective of our work is to use Adaptive Neuro Fuzzy Inference System to predict the daily global solar irradiation for Rabat site. For this purpose, ten models were developed, which differ in the input variables used. Each model uses a different number of variables, ranging from one variable for M1 to a combination of 10 variables for M10. The used variables are Day number (N_j), Ambient temperature (T), Relative Humidity (H_r), Wind speed (W_s), Wind direction (W_D), Declination (δ), Irradiation outside the atmosphere (G_{oh}), Maximum temperature (T_{max}), Minimum temperature (T_{min}). The obtained models were subjected to a statistical study to determine the one with the least error. The selected model is then used to calculate global daily irradiance values.

2. Materials and Methods

2.1. Description of the Measuring Station

In 2008, the Solar Energy and Environment Laboratory of the Faculty of Sciences in Rabat installed a network of measuring stations throughout Morocco (**Figure 1**). One of these stations is in Rabat, which is 75 m above sea level. The climate in Rabat is temperate, with rainfall mainly in winter and relatively little in summer, the average annual temperature in Rabat is 17.9 °C and the annual precipitation is 523 mm per year. In the Rabat measuring station, measurements

are made of the different components of solar radiation and climatic variations. These measurements are carried out by the following instruments^[19–22]:

- Kipp & Zonen SP-Lite pyranometer for global solar radiation measurements (accuracy 2%). The same type of instrument was used to measure the diffuse, but with a sunshield to mask the direct.
- Eppley type pyr heliometer mounted on a tracker to measure direct solar radiation (accuracy 0.5%).
- Total Ultraviolet Radiometer Model TUVR, Eppley type for measuring total solar ultraviolet radiation (accuracy 2%).
- Radiometer type Epply for measuring infra-red radiation (accuracy 0.5%).
- Quantum sensor SKP215, Campbell scientific type for measuring photo-synthetically active radiation PAR (accuracy 0.5%).
- Anemometer with wind vane Model wind monitor 05103, scientific Campbell type for measuring wind speed and direction (accuracy 0.25%).
- Temperature and relative humidity sensor HMP45C manufactured for Campbell Scientific by Vaisala (temperature accuracy 0.2%, humidity accuracy 1%).
- ARG100 rain gauge, manufactured by Environmental Measurements for Campbell Scientific, for rainfall measurement (accuracy 4%).



Figure 1. Solar station of the Solar Energy and Environment Laboratory, Faculty of Science in Rabat.

2.2. Used Data

Global solar irradiance measurements (W/m^2) were taken at 6-minute intervals. The recorded values were averaged to obtain hourly averages of solar irradiance. Then, an integral calculation of these data was performed from

sunrise to sunset, to obtain daily global solar irradiance. Following the same steps, the daily values of the meteorological variables measured at the measuring station were calculated. Thus, the daily evolution of all the climatic variables used in this study is presented in **Figure 2**.

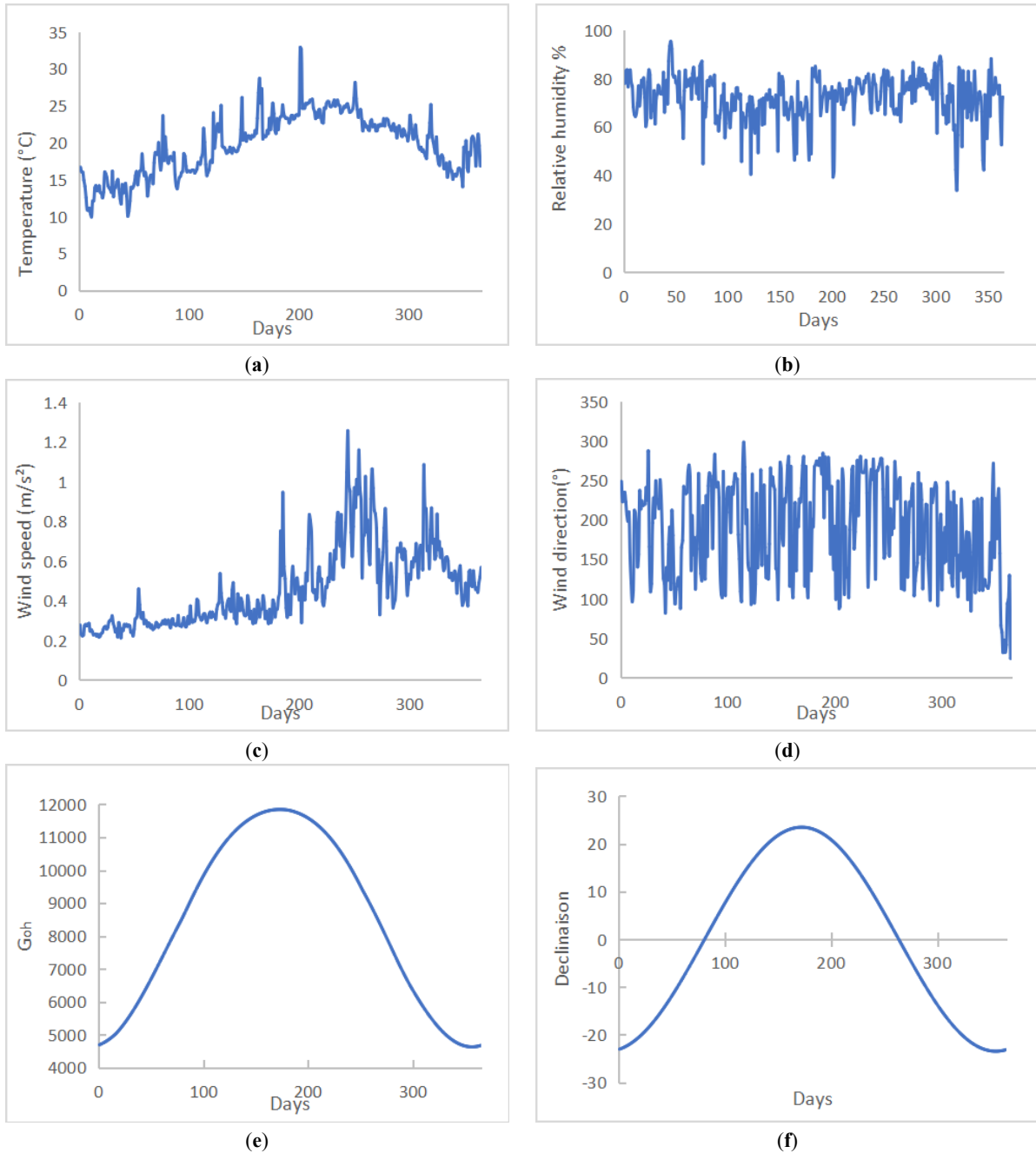


Figure 2. Annual variation of climatic variables. (a) ambient temperature, (b) Relative Humidity (H_r), (c) Wind speed (W_s), (d) Wind direction (W_D), (e) out-of-atmosphere irradiation (G_{oh}), (f) Declination (δ).

2.3. The ANFIS Construction

The classical cycle of developing an ANFIS neuro-fuzzy model can be separated into five steps: Data collection, Analysis and database separation, Selection of a neural network, Training and Validation^[23-25]. The objective of the data collection stage is to collect a sufficient number of data to build a representative database, which will be used to train and test the neural network. This database is the input of the neural network, and consequently it determines both the size of the network and the performance of the system. For our application, we used 10 years of data from 2009 to 2018, (counting 36500 values, 75% for training and 25% for validation) collected by LESE. We worked with weather parameters to forecast global radiation as input: Temperature, Relative Humidity, Wind speed, Wind direction and Declination... and the global radiation as output.

After collecting enough data, it is necessary to proceed to the phase of separating these data into two sets. One part is for training and the other for validation. The separation of the data into two parts (training and testing) is an important element in the evaluation of data estimation models. In general, when we partition data into a training part and a test part, most of the data is used for training and a smaller part of the data is used for testing. The use of similar data for training and testing reduces the errors that lead to misinterpretation of the model results.

The choice of a neural network presents the choice of the architecture of the multilayer neural network. Thus, the solution to a given problem is often achieved by using two approaches: the first one consists in successively adding neurons and connections to a small architecture, and the second one consists in removing neurons and connections from a maximal initial architecture. Both approaches often have the disadvantage of high and unpredictable training times.

During the training process, the weights are adjusted to make the actual (predictive) outputs close to the target (measured) outputs of the network, which are randomly initialized before training, and then iteratively modified to prevent the training from stopping on a local minimum of the error function. The training data set is therefore presented to the network several times with different initialization values for the synaptic weights. Once the architecture of the neural network has been chosen, it must undergo a training phase.

This consists in calculating the optimal weights of the different links, using the training base. When the training of the network is finished, it is always necessary to proceed to validation tests to estimate its quality of generalization by using a different database from the one used for the training. If the performances are not satisfactory, it will be necessary to modify the architecture of the network or to modify the training base.

The statistical learning methods studied in this framework (ANFIS) can be applied in data training, based on the analysis of experimental data. These methods are used for high-level decision systems. ANFIS is a class of adaptive networks proposed by Jang. It can be seen as a non-looped neural network for which each layer is a component of a neuro-fuzzy system. The ANFIS model is the most widely used in practice, used in trajectory tracking, nonlinear approximation, dynamic control, and signal processing^[26-29].

In ANFIS, connections between neurons are only used to specify the direction of propagation of stimuli from other neurons. The structure of ANFIS is composed of five layers, and the if-then rules. ANFIS is one of the earliest neuro-fuzzy systems in existence. It is widely cited in the literature as having proven its effectiveness with its simplified learning algorithm: the gradient descent method and the least squares method^[30-34].

2.4. Choice of the ANFIS Technique for Solar Radiation Estimation

The statistical learning methods studied in ANFIS can be applied in data training based on the analysis of experimental data. These methods are used for high-level decision systems. ANFIS is a class of adaptive networks proposed by Jang. It can be seen as a non-looped neural network for which each layer is a component of a neuro-fuzzy system.

In ANFIS, connections between neurons are only used to specify the direction of propagation of stimulations from other neurons. The ANFIS is one of the earliest neuro-fuzzy systems in existence. It is very cited in the literature because it proved its efficiency with its simplified learning algorithm: the gradient descent method and the least squares method. The structure of ANFIS is composed of five layers^[30-36] as mentioned in **Figure 3**.

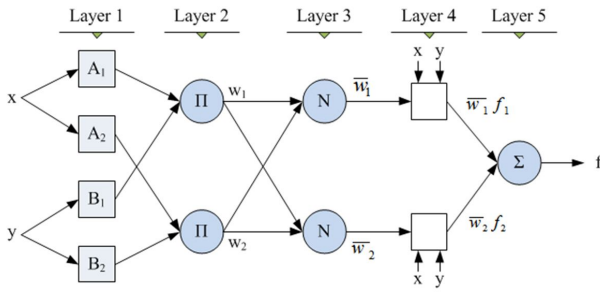


Figure 3. Architecture of an ANFIS.

The First Layer (fuzzification) is the transition from the real world (a voltage, a number, ...) to the fuzzy representation (equation 1). An ANFIS type architecture has as many neurons as there are fuzzy subsets in the represented inference system. Each neuron calculates the truth degree of a particular fuzzy subset by its transfer function. The only restriction on the choice of this function concerns its derivability. In the literature, Gaussian functions are used and the modifiable parameters are the centre and the slope of the Gaussian (variance). The activation function of neurons i in the first layer:

$$f_i^1 = UA_i(x) \tag{1}$$

ponding to variable x . We choose $UA_i(x)$ to be (Gaussian, triangle, trapezoidal) shaped with the maximum equal to 1 and the minimum equal to 0.

The second hidden layer (fuzzy rules) is used to calculate the degree of activation of the premises. The neurons in this layer each represent the premise of a rule. They receive as input the degree of truth of the different fuzzy subsets composing this premise and they are in charge of computing its own degree of truth. The activation functions used for these neurons depend on the operators present in the rules (AND or OR).

In The third hidden layer (normalization), The N neurons are fixed neurons; they perform the normalization of the truth value of the rule (weight) (equation 2).

$$\bar{\omega}_k = \frac{\omega_i}{\omega_1 + \omega_2}, i = 1, 2 \tag{2}$$

while the fourth hidden layer (defuzzification) is the transition from the fuzzy representation to the real representation. This step is used to determine the parameters of the consequence part of the rules (p, q, r). The function of each neuron in this layer is the following (equation 3):

$$f_k^4 = \bar{\omega}_k * f_k = \bar{\omega}_k * (p_k x + q_k y + r_k) \tag{3}$$

Where $\bar{\omega}_k$ is the output of the third layer The parameters p_k, q_k, r_k are called consequence parameters.

Finally, the output layer (The neuron in layer 5) is a fixed neuron, to a given input, it outputs the network response given by (equation 4):

$$f_k^5 = \sum_k \bar{\omega}_k * f_k \tag{4}$$

2.5. Statistical Indicators Used for the Evaluation of the Model's Performance

To quantitatively evaluate the performance of the developed ANFIS models the following statistical indicators were used^[37-41]:

- **RMSE (Root Mean Square Error).** The square root of the root mean square error, RMSE provides information on the short-term performance which is a measure of the variation of the predictive values around the measured data. The lower the RMSE, the more accurate the estimate (equation 5).

$$RMSE = 100 \frac{\sum_{i=0}^n (p_i - m_i)}{\sum_{i=0}^n m_i} \tag{5}$$

- **R² (The correlation coefficient).** The quality of a fit is defined as the quality of a correlation obtained by regression or statistical means using measured values. It depends mainly on the method used (e.g., the least squares method). The most important indicator that determines the quality of the fit is the correlation coefficient R² defined by (equation 6):

$$R^2 = 1 - \frac{RMSE^2}{\sigma^2} \tag{6}$$

Where σ is the standard deviation.

R² can have values between 0 and 1. If it is close to 1 it means that we have a better result from the regression.

- **Average absolute error** measures the average size of deviations, it is always positive (equation 7).

$$MAE = \frac{\sum_{i=0}^n |p_i - m_i|}{N} \tag{7}$$

3. Results and Discussion

3.1. Evaluation of the Relationship between the Input Variable and Global Solar Radiation

In order to visualize the relationship between meteorological parameters and solar irradiation, a graphical rep-

resentation of, number of days (N_j), ambient temperature, Relative Humidity (H_r), Wind speed (W_s), Wind direction (W_D), Declination (δ), out-of-atmosphere irradiation (G_{oh}), maximum sunshine duration (S_0), maximum temperature (T_{max}), minimum temperature (T_{min}), as a function of the

global irradiation was made the obtained results was shown in **Figure 4**.

To quantify the relationship between solar radiation and climatic variables, the correlation coefficient was calculated for each graph in **Figure 4**. The results are shown in **Table 1**.

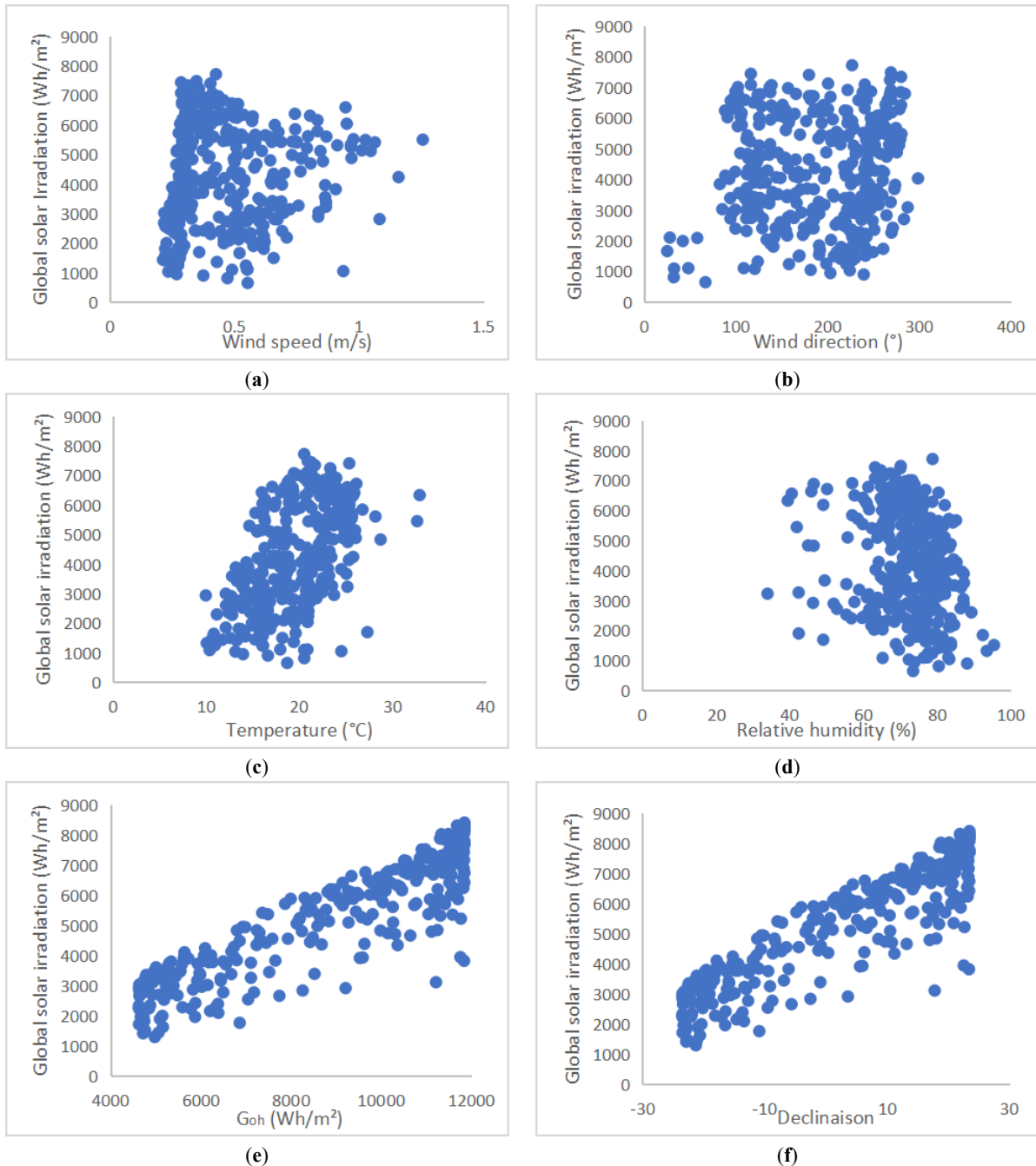


Figure 4. Graphical representation of daily global irradiation as a function of climate variables. (a) Wind speed (W_s), (b) Wind direction (W_D), (c) ambient temperature, (d) Relative Humidity (H_r), (e) out-of-atmosphere irradiation (G_{oh}), (f) Declinaison (δ).

Table 1. Correlation coefficient values relating global irradiation to climate variables.

Input Variables	Correlation Coefficient R ²
Wind direction	0.14
Wind speed	0.18
Relative Humidity	0.24
Temperature	0.57
Declination	0.9
G _{oh}	0.9

3.2. Models Input Variables

This study aims to develop a model based on ANFIS for predicting global solar radiation for the city of Rabat

and surrounding sites. To achieve this objective, several climatological variables (N_j , T , H_r , δ , W_s , W_d , G_0 , T_{max} , T_{min} and S_0), taken as input variables, were combined. The input variables are added step by step to assess the effect of adding each variable on the quality of the previous mode, to find the most appropriate combination of variables for estimating solar radiation at the site under consideration. The order of the variables does not affect the results because for each model the input variables are injected at the same time.

Then, the errors obtained for each model were evaluated, and finally, the models that we considered interesting were chosen. **Table 2** gives an overview of the input variables of the selected models.

Table 2. Input variables of the different models used for training an ANFIS.

Models	Input Parameters	Nj	T	Hr	δ	Ws	Wd	G0	S0	Tmax	Tmin
M1		X									
M2		X	X								
M3		X	X	X							
M4		X	X	X	X						
M5		X	X	X	X	X					
M6		X	X	X	X	X	X				
M7		X	X	X	X	X	X	X			
M8		X	X	X	X	X	X	X	X		
M9		X	X	X	X	X	X	X	X	X	
M10		X	X	X	X	X	X	X	X	X	X

3.3. Evaluation of Models Performance and Results Discussion

ANFIS models are used to predict the daily global solar radiation for the city of Rabat, using available meteorological parameters (e.g., air temperature, extraterrestrial global solar radiation...). In this context, several models are developed based on different inputs. Therefore, we assumed to combine these inputs to obtain the best possible prediction models. The collected data is divided into two subsets, the first part

(75% of the values) is used for training the models, while the rest (25% of the values) is used to test the performance of the models studied. For each model, the number of neurons in the hidden layers was varied from 1 to 10, and 500 training runs were performed with a different initialization each time, for each of these architectures. Then the number of neurons in the sub-layers was set to the value that gives the minimum error; the statistical results obtained for ANFIS are presented in **Table 3**.

Table 3. Performance of the proposed ANFIS model based on different statistical indicators.

	Training Phase			Testing Phase		
	R ²	RMSE (kW/m ²)	MAE (kW/m ²)	R ²	RMSE (kW/m ²)	MBE (kW/m ²)
M1	0.732	0.296	0.174	0.729	0.301	0.177
M2	0.739	0.290	0.161	0.736	0.292	0.163
M3	0.735	0.294	0.166	0.731	0.298	0.170
M4	0.884	0.189	0.122	0.880	0.190	0.122
M5	0.881	0.192	0.126	0.877	0.194	0.129
M6	0.879	0.198	0.129	0.874	0.198	0.130
M7	0.973	0.133	0.102	0.973	0.138	0.106
M8	0.981	0.107	0.089	0.979	0.117	0.101
M9	0.975	0.129	0.095	0.977	0.136	0.104
M10	0.977	0.130	0.098	0.965	0.140	0.109

In order to further evaluate the quality of the ten ANFIS models, and to have a clear idea of which model has the lowest errors, we have presented the different errors in the learning phase and the training phase in the form of a histogram, as shown in **Figures 5** and **6**.

From **Table 1** we can see that the correlation coefficient relating each variable to the global irradiation is relatively low, especially for wind speed and direction. This means that there is no direct relationship between these variables and the global irradiation. However, this is not the case for out-of-atmosphere irradiation and declination where the R^2 is 0.9.

But by combining these variables and using them as input variables in ANFIS models, we notice that the correlation coefficients increase considerably. This is mainly due to ANFIS which tends to create links between the input variables and the output variables.

On the other hand, from the **Table 3** we can see that there are three groups of models which are visibly distinguished by their performance values (RMSE, MAE and R^2). The first group consists of models with combinations of day number, temperature and relative humidity, these models are not efficient, since the value of R^2 is lower than 0.739 and the MAE error is higher than 0.17 kW/m^2 . On the other hand, when we add the declination as input parameter, the statistical indicator improves which is reflected by the correlation coefficient which varies around 0.88. Thus, we obtained a second group containing three models from M4 to M6. But the addition of G_0 and S_0 gives excellent performances with a MAE value lower than 0.089 Kw/m^2 and an R^2 value equal to 98.1%. Therefore, it can be seen that the maximum sunshine duration S_0 as well as the solar radiation outside the atmosphere G_{0h} improve considerably the performance of the solar radiation estimation models.

Training phase

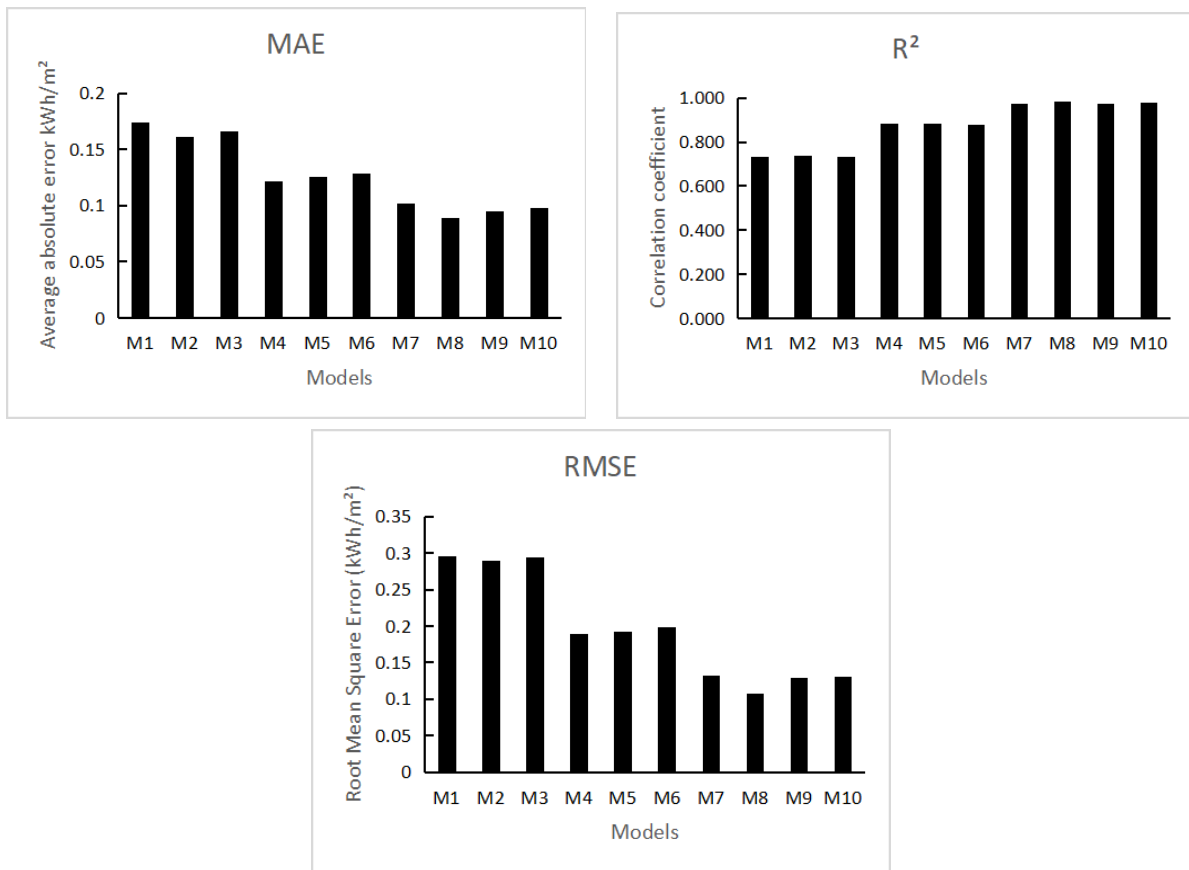


Figure 5. The RMSE, MAE and R^2 for all models in training phase.

Testing phase

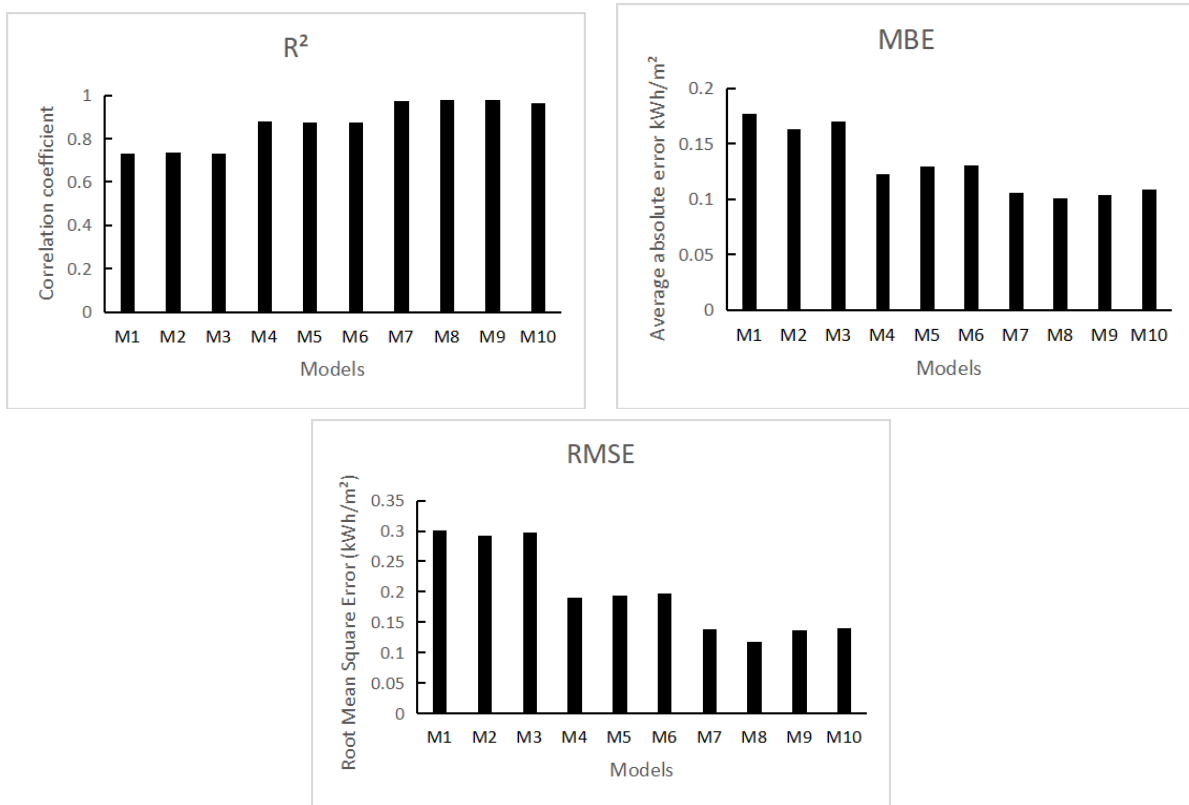


Figure 6. The RMSE, MAE and R² for all models in testing phase.

Comparing the statistical indicators of the different models in both the learning and the testing phase, we can see that the M8 model is the best performing one as it represents the best static indicators. This result is confirmed by the

graphical representation of the estimated values as a function of the measured values of the global irradiation, since it can be seen in Figure 7 that the trend curve almost coincides with the first bisector.

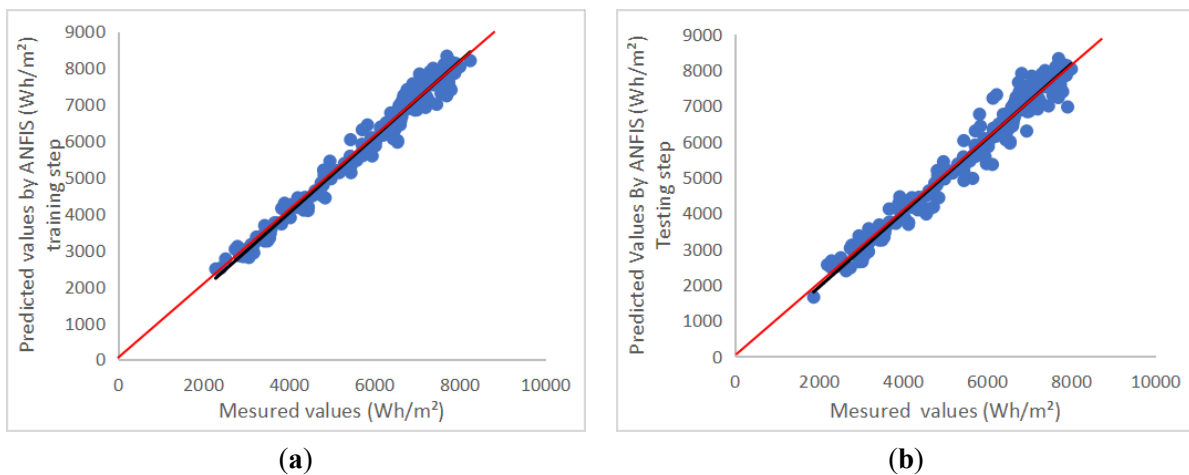


Figure 7. Graphical presentation of the estimated solar irradiation as a function of the measured solar irradiation in the training phase (a) and in the test phase (b).

In our case for the estimation of solar radiation we used the M8 model which is based on the following input variables: day number, temperature, relative humidity, declination, wind speed, wind direction, maximum sunshine duration and solar radiation outside the atmosphere. This choice was made thanks to the statistical indicator which represents the best performance either in the learning phase ($R^2 = 0.981$, $RMSE = 0.107$ kW/m², $MAE = 0.089$ kW/m²) or in the validation phase ($R^2 = 0.979$, $RMSE = 0.117$ kW/m², $MAE = 0.101$ kW/m²). In addition, the annual variation of the estimated and measured solar irradiation is presented in

Figure 8.

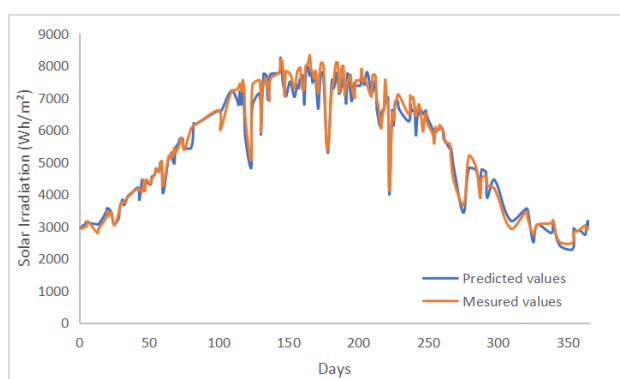


Figure 8. The annual variation of the estimated and measured solar irradiation.

We can see that the difference between the measured data and the predicted values is very small, except for a few days, the difference can be explained either by a bad weather day or by another very unpredictable phenomenon.

4. Conclusions

The use of solar energy requires knowledge of the potential of solar irradiation on horizontal plane. Unfortunately, meteorological stations do not have instruments to measure this fundamental meteorological parameter. This situation motivated us to find new ways of estimating this variable.

In fact, the objective of our study is to develop a model that can be used to predict daily global solar irradiance using ANFIS. For this purpose, ten models have been developed based on different input parameters such as the Day number (N_j), Ambient temperature (T), Relative Humidity (H_r), Wind speed (W_s), Wind direction (W_D), Declination (δ), Irradiation outside the atmosphere (G_{oh}), Maximum temperature (T_{max}), Minimum temperature (T_{min}). In order to select the

most efficient model, three statistical indicators were used (correlation coefficient R^2 , root mean square error RMSE and mean absolute error MAE). The statistical study showed that of the ten models developed, model M8, which takes, day number, temperature, relative humidity, declination, wind speed, wind direction, maximum sunshine duration and solar radiation outside the atmosphere, as input values, has the lowest errors, either in the learning phase ($R^2 = 0.981$, $RMSE = 0.107$ kW/m², $MAE = 0.089$ kW/m²) or in the validation phase ($R^2 = 0.979$, $RMSE = 0.117$ kW/m², $MAE = 0.101$ kW/m²). This result is confirmed by the graphical representation of the estimated values as a function of the measured values of global irradiation, where the trend line coincides with the first bisector. On the other hand, the evolution of daily measured values and estimated values over the year is very similar. All these observations lead to the conclusion that the M8 model is the most suitable for estimating global radiation for the Rabat site and indicates that the applied method is very efficient.

Finally, with the help of this work, it has been possible to develop a valid model for estimating daily global solar radiation for the Rabat site and neighbouring sites. This model will make it possible to quantify the solar energy received at ground level, and it will be an essential tool for researchers in developing and simulating solar thermal and photovoltaic systems. However, it is crucial to complete this work with the prediction of solar irradiation on other time scales (month, season, hour, minute) and to extend this study to the prediction of other components of solar.

Funding

This work received no external funding.

Institutional Review Board Statement

Not applicable.

Informed Consent Statement

Not applicable.

Data Availability Statement

Not applicable.

Acknowledgments

The corresponding author would like to thank the Center for Water, Natural Resources, Environment and Sustainable Development, for their support in participating in carry-

ing out research at the Center.

Conflicts of Interest

The authors declare no conflict of interest.

Nomenclature

N_j	Day number.	T	Ambient temperature.
H_r	Relative Humidity.	W_s	Wind speed.
W_D	Wind direction.	δ	Declination.
G_{oh}	Irradiation outside the atmosphere.	T_{max}	Maximum temperature.
T_{min}	Minimum temperature.	RMSE	Root Mean Square Error.
R^2	Correlation coefficient.	MAE	Average absolute error.

References

- [1] Bahcall, J., 2001. How the Sun shines. *MERCURY-SAN FRANCISCO*. 30(5), 30–37.
- [2] Glaser, P.E., 1968. Power from the sun: Its future. *Science*. 162(3856), 857–861.
- [3] Crabtree, G.W., Lewis, N.S., 2008. Solar energy conversion. In: *AIP Conference Proceedings*. American Institute of Physics. pp. 309–321.
- [4] Kropowski, B., Margolis, R., Ton, D., 2009. Harnessing the sun. *IEEE Power and Energy Magazine*. 7(3), 22–33.
- [5] Cameron, A.G.W., 1958. Nuclear astrophysics. *Annual review of nuclear science*. 8(1), 299–326.
- [6] Salpeter, E.E., 1952. Nuclear reactions in the stars. I. Proton-proton chain. *Physical review*. 88(3), 547.
- [7] Salpeter, E.E., 1953. Energy production in stars. *Annual review of nuclear science*. 2(1), 41–62.
- [8] Broggini, C., Bemmerer, D., Guglielmetti, A., et al., 2010. LUNA: Nuclear astrophysics deep underground. *Annual Review of Nuclear and Particle Science*. 60, 53–73.
- [9] Vernazza, J.E., Avrett, E.H., Loeser, R., 1976. Structure of the solar chromosphere. II-The underlying photosphere and temperature-minimum region. *Astrophysical Journal Supplement Series*. 30, 1–60.
- [10] Bařkal, S., Kim, Y.S., Noz, M.E., 2019. Einstein's $E=mc^2$ Derivable from Heisenberg's Uncertainty Relations. *Quantum Reports*. 1(2), 236–251.
- [11] Grevesse, N., Sauval, A.J., 1998. Standard solar composition. *Space Science Reviews*. 85, 161–174.
- [12] Osterbrock, D.E., 1961. The Heating of the Solar Chromosphere, Plages, and Corona by Magnetohydrodynamic Waves. *The Astrophysical Journal*. 134, 347.
- [13] Rozsnyai, B.F., 2001. Solar opacities. *Journal of Quantitative Spectroscopy and Radiative Transfer*. 71(2–6), 655–663.
- [14] El Mghouchi, Y., Ajzoul, T., El Bouardi, A., 2016. Prediction of daily solar radiation intensity by day of the year in twenty-four cities of Morocco. *Renewable and Sustainable Energy Reviews*. 53, 823–831.
- [15] Nfaoui, H., Buret, J., 1993. Estimation of daily and monthly direct, diffuse and global solar radiation in Rabat (Morocco). *Renewable Energy*. 3(8), 923–930.
- [16] Cantoni, R., Rignall, K., 2019. Kingdom of the Sun: a critical, multiscale analysis of Morocco's solar energy strategy. *Energy Research & Social Science*. 51, 20–31.
- [17] Loutfi, H., Bernatchou, A., Tadili, R., 2017. Generation of horizontal hourly global solar radiation from exogenous variables using an artificial neural network in Fes (Morocco). *International Journal of Renewable Energy Research*. 7(3), 11.
- [18] Berrada, A., Laasmi, M.A., 2021. Technical-economic and socio-political assessment of hydrogen production from solar energy. *Journal of Energy Storage*. 44, 103448.
- [19] Benchrifa, M., Tadili, R., Idrissi, A., et al., 2021. Development of new models for the estimation of hourly components of solar radiation: Tests, comparisons, and application for the generation of a solar database in Morocco. *International Journal of Photoenergy*. 2021, 1–16.
- [20] Benchrifa, M., Essalhi, H., Tadili, R., et al., 2019. Development of a daily databank of solar radiation components for Moroccan territory. *International Journal of Photoenergy*. 2019.
- [21] Benchrifa, M., Mabrouki, J., Essalhi, H., 2023. Estimation of Global Irradiation on Horizontal Plane Using Artificial Neural Network. In: *Artificial Intelligence and Smart Environment: ICAISE'2022*. Springer International Publishing: Cham, Switzerland. pp. 395–400.
- [22] Benchrifa, M., Essalhi, H., Tadili, R., et al., 2022. Estimation of Daily Direct Solar Radiation for Rabat. In: *Sustainable Energy Development and Innovation: Selected Papers from the World Renewable Energy Congress (WREC) 2020*. Springer International Publishing: Cham, Switzerland. pp. 629–634.

- [23] Benchrif, M., Mabrouki, J., Elouardi, M., et al., 2024. Experimental Study of a New Mixed Solar Dryer Design Case Study: Tomato Drying. In: *Technical and Technological Solutions Towards a Sustainable Society and Circular Economy*. Springer Nature: Cham, Switzerland. pp. 557–565. DOI: https://doi.org/10.1007/978-3-031-56292-1_44
- [24] Benchrif, M., Mabrouki, J., Elouardi, M., et al., 2024. Studying the Effect of Integration Intelligent Dust Detection and Cleaning System on the Efficiency of Monocrystalline Photovoltaic Panels. In: *Technical and Technological Solutions Towards a Sustainable Society and Circular Economy*. Springer Nature: Cham, Switzerland. pp. 159–169. DOI: https://doi.org/10.1007/978-3-031-56292-1_12
- [25] Benchrif, M., Mabrouki, J., Ariss, A., et al., 2024. Study of the Physicochemical Properties of Lavender Essential Oil (*Lavandula Stoechas*). In: *Advanced Systems for Environmental Monitoring, IoT and the application of Artificial Intelligence*. Springer Nature: Cham, Switzerland. pp. 329–341. DOI: https://doi.org/10.1007/978-3-031-50860-8_20
- [26] Qazi, A., Fayaz, H., Wadi, A., et al., 2015. The artificial neural network for solar radiation prediction and designing solar systems: a systematic literature review. *Journal of Cleaner Production*. 104, 1–12.
- [27] Elsherikh, A.H., Sharshir, S.W., Abd Elaziz, M., et al., 2019. Modeling of solar energy systems using artificial neural network: A comprehensive review. *Solar Energy*. 180, 622–639.
- [28] Dorvlo, A.S., Jervase, J.A., Al-Lawati, A., 2002. Solar radiation estimation using artificial neural networks. *Applied Energy*. 71(4), 307–319.
- [29] Mohandes, M., Rehman, S., Halawani, T.O., 1998. Estimation of global solar radiation using artificial neural networks. *Renewable energy*. 14(1–4), 179–184.
- [30] Halabi, L.M., Mekhilef, S., Hossain, M., 2018. Performance evaluation of hybrid adaptive neuro-fuzzy inference system models for predicting monthly global solar radiation. *Applied energy*. 213, 247–261.
- [31] Zou, L., Wang, L., Xia, L., et al., 2017. Prediction and comparison of solar radiation using improved empirical models and Adaptive Neuro-Fuzzy Inference Systems. *Renewable energy*. 106, 343–353.
- [32] Alsharif, M.H., Younes, M.K., 2019. Evaluation and forecasting of solar radiation using time series adaptive neuro-fuzzy inference system: Seoul city as a case study. *IET Renewable Power Generation*. 13(10), 1711–1723.
- [33] Sumithira, T.R., Nirmal Kumar, A., 2012. Prediction of monthly global solar radiation using adaptive neuro fuzzy inference system (ANFIS) technique over the State of Tamilnadu (India): a comparative study. *Applied Solar Energy*. 48, 140–145.
- [34] Claywell, R., Nadai, L., Felde, I., et al., 2020. Adaptive neuro-fuzzy inference system and a multilayer perceptron model trained with grey wolf optimizer for predicting solar diffuse fraction. *Entropy*. 22(11), 1192.
- [35] Mohanty, S., 2014. ANFIS based prediction of monthly average global solar radiation over Bhubaneswar (State of Odisha). *Int. J. Ethics Eng. Manag. Educ.* 1(5), 97–101.
- [36] Mohammadi, K., Shamshirband, S., Tong, C.W., et al., 2015. Potential of adaptive neuro-fuzzy system for prediction of daily global solar radiation by day of the year. *Energy Conversion and Management*. 93, 406–413.
- [37] Mabrouki, J., Azrou, M., Dhiba, D., et al., 2021. IoT-based data logger for weather monitoring using arduino-based wireless sensor networks with remote graphical application and alerts. *Big Data Mining and Analytics*. 4(1), 25–32.
- [38] Mabrouki, J., Azrou, M., Fattah, G., et al., 2021. Intelligent monitoring system for biogas detection based on the Internet of Things: Mohammedia, Morocco city landfill case. *Big Data Mining and Analytics*. 4(1), 10–17.
- [39] Mabrouki, J., Fattah, G., Al-Jadabi, N., et al., 2021. Study, simulation and modulation of solar thermal domestic hot water production systems. *Modeling Earth Systems and Environment*. 1–10.
- [40] Mabrouki, J., Azrou, M., Farhaoui, Y., et al., 2020. Intelligent system for monitoring and detecting water quality. In: *Big Data and Networks Technologies 3*. Springer International Publishing. pp. 172–182.
- [41] Mabrouki, J., Benchrif, M., Ennouhi, M., et al., 2023. Geographic Information System for the Study of Water Resources in Chaâba El Hamra, Mohammedia (Morocco). In: *Artificial Intelligence and Smart Environment: ICAISE' 2022*. Springer International Publishing: Cham. pp. 469–474.